

SCIENTIFIC REPORTS



OPEN

A Method for Combined Retinal Vascular and Tissue Oxygen Tension Imaging

Anthony E. Felder^{1,2}, Justin Wanek², Michael R. Tan², Norman P. Blair² & Mahnaz Shahidi³

The retina requires adequate oxygenation to maintain cellular metabolism and visual function. Inner retinal oxygen metabolism is directly related to retinal vascular oxygen tension (PO_2) and inner retinal oxygen extraction fraction (OEF), whereas outer retinal oxygen consumption (QO_2) relies on oxygen availability by the choroid and is contingent upon retinal tissue oxygen tension (tPO_2) gradients across the retinal depth. Thus far, these oxygenation and metabolic parameters have been measured independently by different techniques in separate animals, precluding a comprehensive and correlative assessment of retinal oxygenation and metabolism dynamics. The purpose of the current study is to report an innovative optical system for dual oxyphor phosphorescence lifetime imaging to near-simultaneously measure retinal vascular PO_2 and tPO_2 in rats. The use of a new oxyphor with different spectral characteristics allowed differentiation of phosphorescence signals from the retinal vasculature and tissue. Concurrent measurements of retinal arterial and venous PO_2 , tPO_2 through the retinal depth, inner retinal OEF, and outer retinal QO_2 were demonstrated, permitting a correlative assessment of retinal oxygenation and metabolism. Future application of this method can be used to investigate the relations among retinal oxygen content, extraction and metabolism under pathologic conditions and thus advance knowledge of retinal hypoxia pathophysiology.

The retinal tissue requires an adequate supply of oxygen for cellular metabolism and function. Retinal ischemia due to reduced blood flow has been implicated in the development of vision threatening pathologies such as neovascularization and macular edema^{1,2}. Furthermore, inadequate oxygen availability can lead to hypoxic injury and eventual cell death. Therefore, assessment of retinal oxygenation is essential to improve knowledge of disease pathophysiology and advance treatments that target alleviation of hypoxia-induced pathologies.

Several techniques have become available for quantitative assessment of oxygen content within the retinal vasculature or tissue. Specifically, retinal oximetry for measurement of hemoglobin oxygen saturation (SO_2) has been performed by spectrophotometry³⁻⁵, photoacoustic ophthalmoscopy⁶, and visible optical coherence tomography^{7,8}. Additionally, retinal vascular oxygen tension (PO_2) has been reported using phosphorescence lifetime imaging⁹⁻¹¹. Direct depth-resolved measurements of retinal tissue oxygen tension (tPO_2) have been provided by the oxygen-sensitive microelectrode technique at single point locations¹²⁻¹⁴ and by phosphorescence lifetime imaging at multiple contiguous locations¹⁵. Furthermore, information about the metabolic activity of the retinal tissue has become available by calculation of inner retinal oxygen extraction fraction (OEF) based on retinal vascular oxygen content^{5,16} and by estimation of outer retinal oxygen consumption (QO_2) from retinal tPO_2 depth profiles^{14,17,18}.

To date, these parameters of retinal oxygenation and metabolism have been measured independently in separate animals. Thus, current techniques precluded the assessment of relations among these parameters in the same animal under physiological or pathological conditions which is essential to improve understanding of retinal ischemia pathophysiology. Retinal hypoxia is implicated in the development of vision-threatening retinal pathologies, yet there are currently no direct methods to measure tPO_2 in humans. Alterations in inner retinal OEF due to hypoxia¹⁶ and retinal disease¹⁹ have been demonstrated, but the relationship between tPO_2 and OEF is not known. Furthermore, although presumed, a correspondence between inner retinal tPO_2 and venous PO_2 has not been established. Measurements of these parameters in separate animals cannot accurately

¹Department of Bioengineering, University of Illinois at Chicago, Chicago, IL, 60607, USA. ²Department of Ophthalmology and Visual Science, University of Illinois at Chicago, Chicago, IL, 60612, USA. ³Department of Ophthalmology, University of Southern California, Los Angeles, CA, 90033, USA. Correspondence and requests for materials should be addressed to M.S. (email: mshahidi@usc.edu)

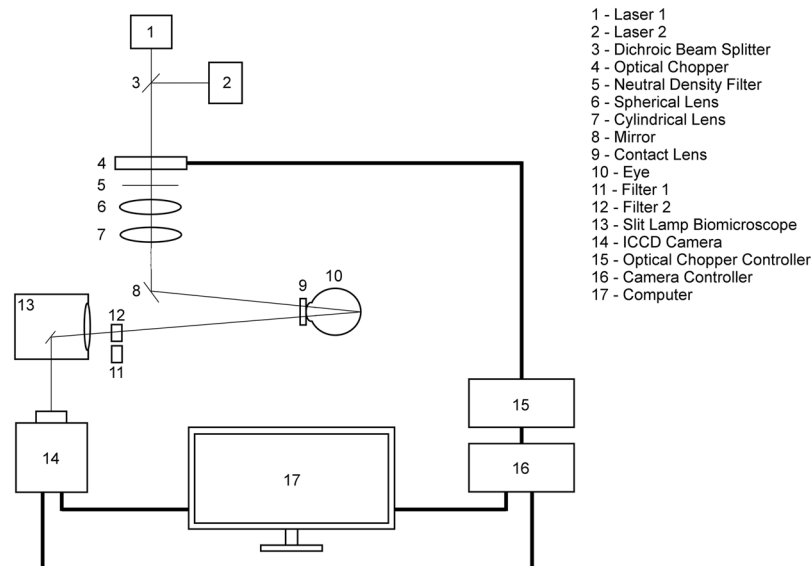


Figure 1. Schematic diagram of the optical imaging system for near-simultaneous measurement of retinal vascular and tissue oxygen tension. Thick lines represent physical connections between system components and thin lines represent the optical path.

determine the association between them due to physiological variations among animals. Therefore, concurrent measurements of retinal vascular PO_2 and tPO_2 in the same animals are necessary to infer reduced tPO_2 based on altered OEF or venous PO_2 under retinal ischemic conditions. These findings may be translated to humans to assess retinal hypoxia and identify OEF thresholds necessary to sustain tPO_2 . The purpose of the current study is to report an innovative optical system for dual oxyphor phosphorescence lifetime imaging to near-simultaneously measure retinal vascular PO_2 and tPO_2 in rats, derive OEF and QO_2 , and determine associations among these parameters.

Methods

Animals. All experimental procedures were in compliance with the ARVO Statement for the Use of Animals in Ophthalmic and Vision Research and approved by the Animal Care Committee of the University of Illinois at Chicago. The study was performed in 10 Long Evans pigmented rats. Rats were anesthetized with intraperitoneal injections of ketamine (100 mg/kg) and xylazine (5 mg/kg) and additional injections were given as required to maintain anesthesia. One day prior to imaging, oxyphor G2 (Oxygen Enterprises, Philadelphia, PA) was constituted at $1.5 \mu\text{M}$ and administered as a $5 \mu\text{L}$ intravitreal bolus injection for retinal tPO_2 imaging. Immediately prior to imaging, oxyphor R0 (Frontier Scientific, Logan, Utah) was administered intravenously (20 mg/kg) for retinal vascular PO_2 imaging. Before imaging, pupils were dilated with 2.5% phenylephrine and 1% tropicamide, and a glass cover slip with 1% hydroxypropyl methylcellulose was placed on the cornea to minimize corneal refractive power and prevent dehydration. Rats were placed on an animal holder with a closed-loop water heater to maintain body temperature at 37°C and were spontaneously breathing during imaging. One eye of each rat was imaged in temporal or nasal regions within three-disk diameters (600 microns) from the edge of the optic nerve head.

Phosphorescence Lifetime Imaging. Our previously established optical imaging system^{9,15} for either retinal vascular PO_2 or tPO_2 measurement was modified for near-simultaneous measurement of both parameters by dual oxyphor phosphorescence lifetime imaging (Fig. 1). The use of two oxyphors (R0 and G2) with different absorption and emission spectra allowed differentiation of phosphorescence signal from within the retinal vasculature and tissue. Two diode lasers at 532 nm (Lasermate Group, Inc. MGM-10) and 635 nm (Lasermate Group, Inc. LTC6358AH) were incorporated into the imaging system for excitation of R0 and G2 oxyphors, respectively. The power of each laser was adjusted to $120 \mu\text{W}$ at the cornea. Both lasers were projected at an oblique angle to the imaging axis and focused to a co-localized 1 mm vertical line on the retina. Since the incident lasers were not coaxial with the imaging path, phosphorescence emission through the retinal depth appeared laterally displaced on the optical section phosphorescence image. A high pass ($>650 \text{ nm}$; Thorlabs, Inc.) or bandpass filter ($810 \pm 25 \text{ nm}$; Midwest Optical Systems, Inc.) was placed interchangeably in the imaging path to selectively image the phosphorescence emission of R0 (within the retinal vasculature) or G2 (within the retinal tissue), respectively. Both lasers were modulated by an optical chopper at 1.6 kHz. Optical section phosphorescence images were acquired by an intensified charge-coupled device (ICCD) camera, while the gain of the intensifier was modulated by the camera software at the same frequency. The optical chopper frequency, ICCD gain modulation frequency and temporal delay increments between the two were selected to produce phase shifts between 0° and 180° . Phosphorescence lifetime was measured from 10 phase-delayed optical section phosphorescence images, as previously described^{9,15}.

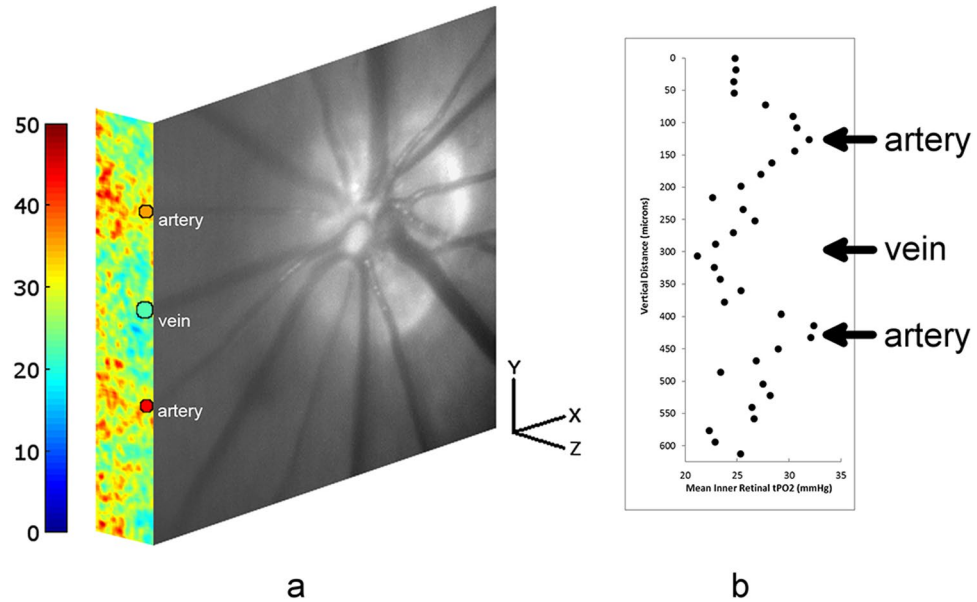


Figure 2. (a) Combined depth-resolved retinal vascular oxygen tension (PO_2) and tissue oxygen tension (tPO_2) images overlaid on the retinal reflectance image in a rat. The vascular PO_2 image displays measurements in two arteries and one vein (labeled), outlined by black circles. Color bar indicates PO_2 in mmHg. (b) Inner retinal tPO_2 plotted along the vertical dimension (superior to inferior) along the tPO_2 image. Locations of the two arteries and one vein are marked.

Image acquisition consisted of imaging G2 and R0 phosphorescence sequentially. First, three repeated phase-delayed optical section phosphorescence images from the retinal tissue were acquired. Then, the excitation laser and emission filter were changed manually (within two seconds) and three repeated phase-delayed optical section phosphorescence images from the retinal vasculature were acquired at exactly the same retinal location. The total time for image acquisition was less than 60 seconds.

Vascular PO_2 and Inner Retinal OEF. Vascular PO_2 in major retinal arteries and veins was measured from the phosphorescence lifetime using the Stern-Volmer equation and the R0 oxyphor's quenching constant and lifetime in a zero-oxygen environment, as previously described^{9,20}. PO_2 in each blood vessel was calculated by averaging three repeated measurements. A mean arterial and venous PO_2 (PO_{2A} and PO_{2V}) was determined for each rat by averaging measurements in each vessel type. Inner retinal OEF was calculated from PO_{2A} and PO_{2V} and using the oxyhemoglobin dissociation curve in rat²¹, as previously described¹⁶. Inner retinal OEF is the fraction of oxygen supplied by the retinal circulation that is extracted by the inner retinal tissue for metabolism, or equivalently, the ratio of inner retinal oxygen metabolism to inner retinal oxygen delivery.

Retinal tPO_2 and Outer Retinal QO_2 . Retinal tissue optical section phosphorescence images were first processed to minimize retinal curvature, then smoothed in vertical (y-axis) and axial (z-axis) dimensions using a 2D anisotropic averaging filter (6×4 pixels), corresponding to $18 \mu\text{m}$ in both axes. A depth-resolved tPO_2 image was generated from the phosphorescence lifetime measured at each pixel using the Stern-Volmer equation and the G2 oxyphor's quenching constant and lifetime in a zero-oxygen environment²², as previously described¹⁵. A mean depth-resolved retinal tPO_2 image was generated from three repeated images.

Along the vertical dimension of each retinal tPO_2 image (superior to inferior), 35 contiguous tPO_2 depth profiles were generated by vertically averaging tPO_2 over 10 pixels (30 microns) and plotting tPO_2 as a function of retinal depth, as previously described¹⁵. The outer and inner retina were defined as 50% to 100% and 0% to 50% of the retinal depth, respectively. Maximum outer retinal tPO_2 , minimum outer retinal tPO_2 , and mean inner retinal tPO_2 were calculated from each tPO_2 depth profile. Mean inner retinal tPO_2 was plotted along the vertical dimension of the image to demonstrate changes in this parameter with respect to retinal arteries and veins. Furthermore, mean values for each parameter were calculated from all profiles along the tPO_2 image.

From each retinal tPO_2 depth profile, outer retinal QO_2 was calculated by fitting a three-layer, one-dimensional, steady-state oxygen diffusion model using a non-linear least squares technique, as previously described^{12,14,17,23}. In this model, oxygen diffuses in one dimension from the choroidal circulation across the outer retinal depth, which is divided into three layers¹⁴, based on their oxygen consumption properties. QO_2 has been shown to be negligible in layers 1 and 3²³, which correspond to the photoreceptor outer segments and outer nuclear layer, respectively. In contrast, oxygen is consumed in layer 2 by mitochondria of the photoreceptor inner segments, yielding a quadratic relationship between tPO_2 and retinal depth. A mean outer retinal QO_2 was calculated by averaging measurements obtained from all tPO_2 depth profiles along the vertical dimension of the tPO_2 image.

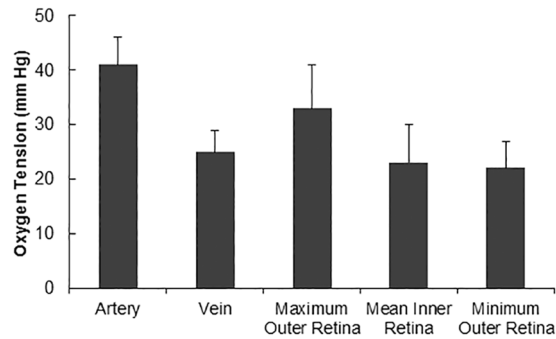


Figure 3. Retinal arterial and venous oxygen tension (PO_2) and tissue oxygen tension (tPO_2) measurements in 10 rats. Error bars indicate standard deviations.

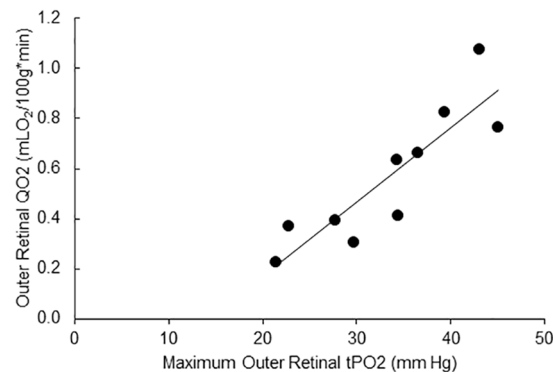


Figure 4. Relationship between outer retinal oxygen consumption (QO_2) and maximum outer retinal tissue oxygen tension (tPO_2). The regression line best fit to the data is shown ($R^2 = 0.77$).

Data availability. The data generated are available from the corresponding author on reasonable request.

Results

A representative example of a retinal vascular PO_2 and tPO_2 image obtained at the same location overlaid on the retinal reflectance image is shown in Fig. 2a. The vascular PO_2 image displays measurements in two arteries and one vein, demonstrating higher PO_{2A} than PO_{2V} , as expected. The tPO_2 image shows higher tPO_2 near the chorioretinal interface compared to inner retina. Mean inner retinal tPO_2 plotted along the vertical dimension (superior to inferior) is shown in Fig. 2b, displaying higher tPO_2 near arteries than the vein.

Compiled retinal vascular PO_2 and tPO_2 measurements in all rats are presented in Fig. 3. PO_{2A} and PO_{2V} were 41 ± 5 mmHg and 25 ± 4 mmHg, respectively ($P < 0.001$; $N = 10$). Inner retinal tPO_2 , minimum outer retinal PO_2 , maximum outer retinal PO_2 were 23 ± 7 mmHg, 22 ± 5 mmHg and 33 ± 8 mmHg, respectively. There was no significant difference between PO_{2V} and mean inner retinal tPO_2 ($P = 0.4$). Inner retinal OEF was 0.58 ± 0.11 and outer retinal QO_2 was 0.57 ± 0.27 mLO₂/100 g*min. There was no significant correlation between inner retinal OEF and mean inner retinal tPO_2 ($R^2 = 0.05$; $P = 0.53$; $N = 10$). As demonstrated in Fig. 4, there was a significant correlation between outer retinal QO_2 and maximum outer retina tPO_2 ($R^2 = 0.77$; $P < 0.001$; $N = 10$).

Discussion

A novel optical imaging method for near-simultaneous imaging of retinal vascular PO_2 and tPO_2 was demonstrated by phosphorescence lifetime imaging of dual oxyphors delivered intravenously and intravitreally. For the first time, concurrent assessment of oxygen content across the retinal depth and oxygen metabolism metrics of the inner and outer retina was demonstrated. Future application of this method can provide knowledge of relations among these parameters under experimental pathologic conditions and thus yield a comprehensive understanding of retinal oxygenation and metabolism dynamics.

Measurements of retinal PO_{2A} and PO_{2V} were in general agreement with those from previous studies^{24, 25}. Depth-resolved retinal tPO_2 images displayed maximum tPO_2 near the choroid, consistent with normal physiology. Inner retinal tPO_2 measurements using the G2 oxyphor were similar to our previously published data with the R2 oxyphor¹⁵ and those reported by the oxygen microelectrode technique¹⁴. Alterations in inner retinal tPO_2 were consistent with the nearby presence of arteries and veins. Inner retinal OEF was 0.58, on average, indicating 58% of the oxygen delivered by the retinal circulation was extracted for metabolism by the inner retinal tissue. The mean inner retinal OEF was higher as compared to our previous study¹⁶ and maximum outer retinal tPO_2 in the current study was slightly lower than previous reports^{14, 15}. Both of these results are consistent with the

presence of reduced systemic oxygenation²⁶, which likely resulted from the effect of anesthesia while the rats were under spontaneous breathing conditions²⁷. Furthermore, the variability of tPO₂ adjacent to the chorioretinal interface along the tPO₂ image may, at least in part, be attributed to presumed anesthesia-induced systemic hypotension. This may have resulted in reduced choroidal blood flow, thus altering tPO₂ gradients within the retinal depth. Overall, the results demonstrate the ability of the optical imaging system to measure retinal vascular PO₂, tPO₂ and inner retinal OEF.

Measurements of outer retinal QO₂ obtained in the current study were similar to our previously reported values¹⁷, but lower than those obtained by the oxygen microelectrode technique in light-adapted rats^{12, 14, 18}. This difference is likely due to intraretinal phosphorescence scattering which decreases the depth resolution, minimizes the curvature of tPO₂ profiles and calculated values of QO₂. Nevertheless, outer retinal QO₂ was significantly associated with maximum outer retinal tPO₂, in agreement with a previous study¹⁴, though a small portion of oxygen utilized by the photoreceptors is supplied by the retinal vasculature¹⁴. This result suggests a dependence of the photoreceptor metabolic function on the level of oxygen supplied by the choroidal circulation.

Simultaneous measurements of retinal vascular PO₂ and tPO₂ coupled with derivation of inner retina OEF and outer retinal QO₂ can advance knowledge of retinal oxygen dynamics. For example, we demonstrated here, for the first time, that there was no significant correlation between inner retinal OEF and mean inner retinal tPO₂ under healthy condition. This result suggests that despite physiological variations, tPO₂ is well-maintained due to compensatory alterations in OEF and oxygen delivery, and implies the presence of highly effective regulatory mechanisms. Previous studies have shown alterations in OEF under experimental hypoxia in rats¹⁶. In future studies, by relating inner retinal tPO₂ with OEF under graded hypoxia/ischemia, diabetes or light flicker stimulation, the OEF threshold necessary to sustain tPO₂ may be identified. Additionally, data obtained under graded levels of ischemia may be used to establish a relationship between inner retinal tPO₂ and PO_{2v}. Furthermore, combined retinal blood flow measurements with the current method can be used to determine the inner retinal oxygen delivery threshold necessary to maintain retinal tPO₂ with direct relevance to retinal ischemic diseases. These thresholds can only be accurately determined with concurrent retinal vascular PO₂ and tPO₂ measurements in the same animal.

One potential limitation of this method is the scattering of phosphorescence light within the retina and vitreous which can degrade image quality. However, compared to the R2 oxyphor, less scattering is expected from the G2 oxyphor due to its longer phosphorescence emission wavelength. The quenching constants used to calculate PO₂ were obtained from literature and may be different within the retinal tissue environment. Phototoxicity may affect data derived from images acquired repeatedly at the same location with R0 oxyphor²⁸, but any effect of phototoxicity on measurements derived using the G2 oxyphor is not known. Although, the laser irradiance was below the threshold for tissue damage, repeatability of measurements obtained at the same location with the use of dual oxyphors will need further evaluation. The feasibility of the method was demonstrated in a limited number of rats and future studies using larger sample sizes are needed to fully establish the utility of the method.

In conclusion, for the first time, near-simultaneous measurement of retinal vascular and tissue oxygen tension by phosphorescence lifetime imaging was demonstrated. Future application of this method under challenged physiologic or pathologic conditions permits correlation of retinal vascular and tissue oxygen content and can potentially elucidate retinal oxygenation dynamics.

References

- Campochiaro, P. A. Molecular pathogenesis of retinal and choroidal vascular diseases. *Progress in retinal and eye research* **49**, 67–81, doi:10.1016/j.preteyeres.2015.06.002 (2015).
- Kurihara, T., Westenskow, P. D. & Friedlander, M. Hypoxia-inducible factor (HIF)/vascular endothelial growth factor (VEGF) signaling in the retina. *Advances in experimental medicine and biology* **801**, 275–281, doi:10.1007/978-1-4614-3209-8_35 (2014).
- Olafsdottir, O. B., Eliasdottir, T. S., Kristjansdottir, J. V., Hardarson, S. H. & Stefansson, E. Retinal Vessel Oxygen Saturation during 100% Oxygen Breathing in Healthy Individuals. *PLoS one* **10**, e0128780, doi:10.1371/journal.pone.0128780 (2015).
- Hammer, M., Vilser, W., Riemer, T. & Schweitzer, D. Retinal vessel oximetry-calibration, compensation for vessel diameter and fundus pigmentation, and reproducibility. *Journal of Biomedical Optics* **13**, doi:10.1117/1.2976032 (2008).
- Felder, A. E., Wanek, J., Blair, N. P. & Shahidi, M. Inner Retinal Oxygen Extraction Fraction in Response to Light Flicker Stimulation in Humans. *Invest Ophthalmol Vis Sci* **56**, 6633–6637, doi:10.1167/iovs.15-17321 (2015).
- Song, W. et al. A combined method to quantify the retinal metabolic rate of oxygen using photoacoustic ophthalmoscopy and optical coherence tomography. *Sci Rep* **4**, 6525, doi:10.1038/srep06525 (2014).
- Yi, J. et al. Visible light optical coherence tomography measures retinal oxygen metabolic response to systemic oxygenation. *Light, science & applications* **4**, doi:10.1038/lsa.2015.107 (2015).
- Soetikno, B. T. et al. Inner retinal oxygen metabolism in the 50/10 oxygen-induced retinopathy model. *Scientific reports* **5**, 16752, doi:10.1038/srep16752 (2015).
- Shahidi, M., Shakoor, A., Blair, N. P., Mori, M. & Shonat, R. D. A method for chorioretinal oxygen tension measurement. *Curr Eye Res* **31**, 357–366, doi:10.1080/02713680600599446 (2006).
- Blair, N. P., Wanek, J. M., Mori, M. & Shahidi, M. Abnormal retinal vascular oxygen tension response to light flicker in diabetic rats. *Invest Ophthalmol Vis Sci* **50**, 5444–5448, doi:10.1167/iovs.09-3465 (2009).
- Wanek, J., Teng, P. Y., Albers, J., Blair, N. P. & Shahidi, M. Inner retinal metabolic rate of oxygen by oxygen tension and blood flow imaging in rat. *Biomed Opt Express* **2**, 2562–2568, doi:10.1364/BOE.2 (2011).
- Cringle, S. J., Yu, D. Y., Yu, P. K. & Su, E. N. Intraretinal oxygen consumption in the rat *in vivo*. *Invest Ophthalmol Vis Sci* **43**, 1922–1927 (2002).
- Wangsa-Wirawan, N. D. & Linsenmeier, R. A. Retinal oxygen: fundamental and clinical aspects. *Arch Ophthalmol* **121**, 547–557, doi:10.1001/archophth.121.4.547 (2003).
- Lau, J. C. & Linsenmeier, R. A. Oxygen consumption and distribution in the Long-Evans rat retina. *Exp Eye Res* **102**, 50–58, doi:10.1016/j.exer.2012.07.004 (2012).
- Shahidi, M., Wanek, J., Blair, N. P., Little, D. M. & Wu, T. Retinal Tissue Oxygen Tension Imaging in Rat. *Investigative ophthalmology & visual science* 09–4710 (2010).
- Teng, P. Y., Wanek, J., Blair, N. P. & Shahidi, M. Inner retinal oxygen extraction fraction in rat. *Invest Ophthalmol Vis Sci* **54**, 647–651, doi:10.1167/iovs.12-11305 (2013).

17. Wanek, J., Blair, N. P. & Shahidi, M. Outer retinal oxygen consumption of rat by phosphorescence lifetime imaging. *Curr Eye Res* **37**, 132–137, doi:10.3109/02713683.2011.629071 (2012).
18. Yu, D. Y. & Cringle, S. J. Oxygen distribution and consumption within the retina in vascularised and avascular retinas and in animal models of retinal disease. *Progress in retinal and eye research* **20**, 175–208 (2001).
19. Felder, A. E. *et al.* The Effects of Diabetic Retinopathy Stage and Light Flicker on Inner Retinal Oxygen Extraction Fraction. *Invest Ophthalmol Vis Sci* **57**, 5586–5592, doi:10.1167/iovs.16-20048 (2016).
20. Lo, L. W., Koch, C. J. & Wilson, D. F. Calibration of oxygen-dependent quenching of the phosphorescence of Pd-meso-tetra (4-carboxyphenyl) porphine: a phosphor with general application for measuring oxygen concentration in biological systems. *Anal Biochem* **236**, 153–160, doi:10.1006/abio.1996.0144 (1996).
21. Cartheuser, C. F. Standard and pH-affected hemoglobin-O₂ binding curves of Sprague-Dawley rats under normal and shifted P50 conditions. *Comparative biochemistry and physiology. Comparative physiology* **106**, 775–782 (1993).
22. Dunphy, I., Vinogradov, S. A. & Wilson, D. F. Oxyphor R2 and G2: phosphors for measuring oxygen by oxygen-dependent quenching of phosphorescence. *Anal Biochem* **310**, 191–198 (2002).
23. Haugh, L. M., Linsenmeier, R. A. & Goldstick, T. K. Mathematical models of the spatial distribution of retinal oxygen tension and consumption, including changes upon illumination. *Ann Biomed Eng* **18**, 19–36 (1990).
24. Wanek, J., Teng, P. Y., Blair, N. P. & Shahidi, M. Inner retinal oxygen delivery and metabolism under normoxia and hypoxia in rat. *Invest Ophthalmol Vis Sci* **54**, 5012–5019, doi:10.1167/iovs.13-11887 (2013).
25. Yu, D. Y., Cringle, S. J., Alder, V. & Su, E. N. Intraretinal oxygen distribution in the rat with graded systemic hyperoxia and hypercapnia. *Investigative ophthalmology & visual science* **40**, 2082–2087 (1999).
26. Teng, P. Y., Wanek, J., Blair, N. P. & Shahidi, M. Response of Inner Retinal Oxygen Extraction Fraction to Light Flicker Under Normoxia and Hypoxia in Rat. *Investigative Ophthalmology & Visual Science* **55**, 6055–6058, doi:10.1167/iovs.13-13811 (2014).
27. Shakoor, A., Gupta, M., Blair, N. P. & Shahidi, M. Chorioretinal vascular oxygen tension in spontaneously breathing anesthetized rats. *Ophthalmic Res* **39**, 103–107, doi:10.1159/000099246 (2007).
28. Stepinac, T. K. *et al.* Light-induced retinal vascular damage by Pd-porphyrin luminescent oxygen probes. *Investigative ophthalmology & visual science* **46**, 956–966, doi:10.1167/iovs.04-0500 (2005).

Acknowledgements

This study was supported by NIH grants EY017918 and EY001792, Senior Scientific Investigator award (MS) and an unrestricted departmental grant from Research to Prevent Blindness.

Author Contributions

A.E.F.: experimental design, data acquisition, data analysis, data interpretation, writing. J.W.: data analysis, data interpretation, writing. M.R.T.: data acquisition. N.P.B.: data interpretation, writing. M.S.: experimental design, data analysis, data interpretation, writing. All authors reviewed the manuscript.

Additional Information

Competing Interests: The authors declare that they have no competing interests.

Publisher's note: Springer Nature remains neutral with regard to jurisdictional claims in published maps and institutional affiliations.



Open Access This article is licensed under a Creative Commons Attribution 4.0 International License, which permits use, sharing, adaptation, distribution and reproduction in any medium or format, as long as you give appropriate credit to the original author(s) and the source, provide a link to the Creative Commons license, and indicate if changes were made. The images or other third party material in this article are included in the article's Creative Commons license, unless indicated otherwise in a credit line to the material. If material is not included in the article's Creative Commons license and your intended use is not permitted by statutory regulation or exceeds the permitted use, you will need to obtain permission directly from the copyright holder. To view a copy of this license, visit <http://creativecommons.org/licenses/by/4.0/>.

© The Author(s) 2017